GMR
The Original

BIOCOMPATIBLE STARCH/PVA ELECTROSPUN NANOSCAFFOLDS INCORPORATED WITH GREEN-SYNTHESISED OF CuO NANOPARTICLES FROM *Gracilaria corticata* EXTRACT: PHYSICOCHEMICAL CHARACTERIZATION AND ANTICANCER ACTIVITY

Lishya Sri Nagaraj[1], Swetha P[2], Alagendran Subbarayalu[3]

[1]Saveetha Medical College & Hospital (SMCH), Saveetha Institute of Medical and Technical Sciences (SIMATS), Thandalam, Chennai, Tamil Nadu 602105, India. lishya2212@gmail.com
[2]Department of Pathology, Saveetha Medical College and Hospital, Saveetha Institute of Medical And Technical Sciences (SIMATS), Thandalam, Chennai-602105, Tamil Nadu, India. Email: spswethu@gmail.com; ORCID: https://orcid.org/0009-0008-5190-5113.
[3]Clinical Neuroscience and Phytomedicine Laboratory, Department of Research, Saveetha College of Nursing (SCON), Saveetha Institute of Medical and Technical Sciences (SIMATS), Chennai 602105, Tamil Nadu, India. Email: proteinblg@gmail.com; alagendrans.scon@saveetha.com. ORCID: https://orcid.org/0009-0009-0749-7180.
*Correspondence: proteinblg@gmail.com; alagendrans.scon@saveetha.com (A.S.)

ABSTRACT
This study reports the green synthesis of copper oxide nanoparticles (CuO NPs) using *Gracilaria corticata* red algal extract and their incorporation into starch/polyvinyl alcohol (PVA) electrospun nanoscaffolds for enhanced anticancer applications. UV-Vis spectroscopy confirmed nanoparticle formation with a distinct surface plasmon resonance peak at 291 nm, while Fourier-transform infrared spectroscopy (FTIR) analysis revealed functional groups from algal phytochemicals that stabilized the CuO NPs. X-ray diffraction (XRD) confirmed the monoclinic crystalline structure of CuO NPs, and Scanning electron microscopy (SEM) demonstrated uniform fiber morphology (90–150 nm) with well-dispersed nanoparticles. Thermogravimetric analysis (TGA) indicated improved thermal stability, with degradation onset at 265.25°C. Dynamic light scattering (TGA) showed CuO NPs with an average size of 68.6 nm and a zeta potential of -14.11 mV, suggesting moderate colloidal stability. The anticancer efficacy was evaluated against HT-29 (colon cancer) and MCF-7 (breast cancer) cells via MTT assay. The starch/PVA/CuO-NPs nanoscaffolds exhibited the highest cytotoxicity, with IC50 values of ~10 µg/mL (HT-29) and ~20 µg/mL (MCF-7), outperforming standalone CuO NPs (IC50 ~15 µg/mL and ~25 µg/mL, respectively) and algal extract (IC50 ~50 µg/mL and ~40 µg/mL). These results highlight the scaffold's superior anticancer activity, likely due to synergistic effects between CuO NPs and the polymer matrix. The study demonstrates the potential of biocompatible, algae-mediated nanoscaffolds as a promising platform for cancer therapy, warranting further *in vivo* exploration.

KEYWORDS: *Gracilaria corticata*, Green synthesis, CuO nanoparticles, starch/PVA/CuO-NPs nanoscaffolds, Anticancer activity.

1. INTRODUCTION

Nanotechnology has revolutionized the field of biomedical engineering by enabling the development of advanced nanomaterials with unique physicochemical properties tailored for therapeutic applications [1]. Among these, metal oxide nanoparticles have gained considerable attention due to their multifunctional roles in drug delivery, antimicrobial activity, and notably, anticancer therapy [2]. Copper oxide nanoparticles (CuO NPs), in particular, have emerged as promising agents owing to their intrinsic biological activities, including reactive oxygen species (ROS) generation, which can selectively induce cytotoxicity in cancer cells [3]. However, conventional chemical synthesis methods of CuO NPs often involve hazardous reagents and harsh conditions, raising concerns about their biocompatibility and environmental impact [4]. This has catalyzed interest in green synthesis approaches that utilize natural biological resources as reducing and stabilizing agents, offering eco-friendly, cost-effective, and scalable alternatives [5].

Marine macroalgae are a rich and renewable source of diverse bioactive compounds, including polysaccharides, polyphenols, and pigments, which can act as natural reducing agents during nanoparticle synthesis [6]. The red seaweed *Gracilaria corticata* is abundant in coastal regions and has been extensively studied for its pharmacological potentials, including antioxidant, antimicrobial, and anticancer properties [7]. Its unique

biochemical composition makes it an ideal candidate for ultrasonic-assisted extraction (UAE) of bioactive compounds, which improves yield and efficiency by disrupting the algal cell walls through cavitation effects [8]. Incorporating *G. corticata* extracts in nanoparticle synthesis not only facilitates green reduction but also imparts additional biofunctionalities to the resulting nanoparticles [9].

Parallel to the synthesis of functional nanoparticles, the development of biocompatible and biodegradable scaffolds capable of supporting cellular growth and targeted drug delivery remains a cornerstone of tissue engineering and cancer therapeutics [10]. Electrospinning technology has gained prominence for fabricating nanofibrous scaffolds that closely mimic the native extracellular matrix (ECM) architecture [11]. Blending natural polymers like starch, a polysaccharide known for its biodegradability and non-toxic nature, with synthetic polymers such as polyvinyl alcohol (PVA) can yield composite scaffolds that combine mechanical strength with biological compatibility [12]. Starch/PVA electrospun nanofibers offer a hydrophilic environment conducive to cell attachment and proliferation, making them excellent candidates for biomedical applications [13].

Embedding green-synthesized CuO NPs within starch/PVA nanofibrous scaffolds opens new avenues for developing multifunctional platforms that integrate structural support with anticancer activity [14]. This composite approach ensures controlled nanoparticle release and enhanced interaction with cancer cells, improving therapeutic efficacy while minimizing systemic toxicity [15]. Moreover, electrospun nanoscaffolds facilitate sustained bioavailability and localized action of nanoparticles, which is crucial for effective cancer treatment [16]. Despite the potential, there is limited literature exploring the combination of green CuO NPs synthesized from marine algae with starch/PVA nanofibers for anticancer applications, highlighting the novelty and relevance of this research [17].

Physicochemical characterization plays a pivotal role in elucidating the structural, morphological, and thermal properties of synthesized nanomaterials and their composites [18]. Techniques such as UV-Visible spectroscopy confirm nanoparticle formation through characteristic surface plasmon resonance [19], while Fourier-transform infrared (FTIR) spectroscopy reveals molecular interactions and functional group involvement in nanoparticle stabilization and scaffold integration [20]. X-ray diffraction (XRD) analysis provides insights into crystalline phases and purity of CuO NPs, whereas scanning electron microscopy (SEM) visualizes fiber morphology and nanoparticle distribution within the scaffold matrix [21]. Thermal gravimetric analysis (TGA) evaluates thermal stability essential for biomedical applications [22], and dynamic light scattering (DLS) alongside zeta potential measurements ascertain particle size distribution and colloidal stability, which directly influence biological activity and biocompatibility [23].

In vitro anticancer assays using human cancer cell lines such as HT-29 (colon adenocarcinoma) and MCF-7 (breast adenocarcinoma) offer preliminary validation of the therapeutic potential of the synthesized nanocomposites [24]. Evaluating cell viability via MTT assays following treatment with the nanoscaffolds helps determine cytotoxic concentrations and provides mechanistic insights into the mode of action, including ROS-mediated apoptosis or necrosis pathways [25]. The combinational effect of starch/PVA scaffolds and CuO NPs is hypothesized to enhance anticancer efficacy by synergistically leveraging the scaffold's biocompatibility and the nanoparticles' cytotoxicity [26].

This study aims to fabricate biocompatible starch/PVA electrospun nanofibrous scaffolds incorporated with CuO NPs green-synthesized through an UAE process using *G. corticata* extract [27]. The objectives include comprehensive physicochemical characterization to confirm successful nanoparticle synthesis and scaffold integration, and evaluation of anticancer activity against human colon and breast cancer cell lines [28]. The ultrasonic-assisted green synthesis method not only offers an eco-friendly alternative to conventional nanoparticle fabrication but also leverages marine biomass as a sustainable resource [29]. The incorporation of CuO NPs into starch/PVA nanoscaffolds is expected to create a multifunctional material with promising applications in targeted cancer therapy.

2. MATERIALS AND METHODS

2.1 Chemicals and reagents

The brown seaweed *G. corticata* was collected from the coastal region of Rameswaram, Tamil Nadu, India, serving as a green and renewable source for the biosynthesis of CuO NPs. Analytical-grade copper (II) sulfate pentahydrate ($CuSO_4 \cdot 5H_2O$) procured from Merck was employed as the copper ion precursor. PVA, with a molecular weight near 115,000 g/mol, together with starch, was utilized to prepare biocompatible and biodegradable nanofibrous scaffolds. Electrospinning procedures were executed using a HOLMARC HO-NFES-040 apparatus. All other solvents and reagents were obtained from Sigma-Aldrich and Merck, ensuring analytical-grade quality for experimental reproducibility. Characterization techniques for CuO NPs and nanofibrous scaffolds included UV-Visible spectroscopy, FTIR, XRD, SEM, DLS, zeta potential measurements, and TGA. The anticancer potential was evaluated using established *in vitro* bioassays.

2.2 Collection and processing of marine algae

The brown macroalga *G. corticata* was harvested from the intertidal zone along the shores of Rameswaram. Immediately after collection, samples were stored in cooled containers to preserve bioactive compounds. The algal material was thoroughly rinsed with tap water to remove dirt and epiphytes, followed by multiple washes with distilled water to eliminate salt residues. Approximately 100 g of the cleaned seaweed was chopped into small fragments and air-dried at ambient room temperature for two weeks. Once dried, the biomass was pulverized into a fine powder using a mechanical grinder and stored in sealed containers under cool, dry conditions until further use.

2.3 UAE of bioactive compounds

Bioactive molecules were extracted from the powdered *G. corticata* using UAE to improve extraction efficiency by disrupting algal cell walls. A sample of 2 g dried algal powder was suspended in 50 mL Milli-Q water within a 100 mL borosilicate beaker. The suspension was sonicated at 60°C for 45 minutes in a LABQUEST ultrasonic cleaner (Borosil; Serial No. 941032329018). The resulting mixture was filtered through sterilized Whatman No. 1 filter paper, and the clear filtrate was stored at 10°C. A portion of this extract was freeze-dried and reserved for the synthesis of CuO NPs [30, 31].

2.4 Green synthesis of CuO NPs

Biosynthesis of CuO NPs was conducted by mixing the algal extract with a copper salt solution. An aqueous solution of 0.1 M $CuSO_4 \cdot 5H_2O$ (50 mL) was combined with 10 mL of algal extract (10 mg/mL), maintaining a precursor-to-extract volumetric ratio of 5:1. The mixture was stirred magnetically at 650 rpm and heated at 60°C for 2 hours. The shift in color from deep blue to bluish-green indicated the reduction of Cu^{2+} ions mediated by phytochemicals. The CuO NPs formed were washed thrice using double-distilled water and subsequently freeze-dried for 48 hours, yielding a fine powder used for scaffold fabrication and biological assays [32].

2.5 Preparation of starch/PVA nanofibrous scaffolds loaded with CuO NPs

Nanofibrous mats were fabricated by electrospinning a starch-PVA blend infused with biosynthesized CuO NPs. A 15% (w/w) PVA solution was prepared by dissolving the polymer in Milli-Q water under continuous stirring at 50°C. Then, 100 mg starch and 100 mg CuO NPs were incorporated and stirred for 2.5 hours at 50°C to ensure homogeneous mixing. This viscous solution was loaded into a 10 mL syringe fitted with a stainless steel needle (0.84 mm inner diameter). Electrospinning was performed on the HOLMARC HO-NFES-040 instrument with parameters set at 11.5 kV voltage, 12.3 cm needle-to-collector distance, and 0.4 mL/h flow rate. The process occurred at room temperature for 6 to 8 hours. The resultant nanofibrous mats were collected and kept in desiccators to maintain their morphology [33-35].

2.6 Physicochemical characterization

2.6.1 UV-visible spectroscopy

Absorption spectra of the algal extract, synthesized CuO NPs, and CuO-loaded starch/PVA nanofibers were measured using a VIS SPEC V-730 spectrophotometer over the 200–800 nm wavelength range. Deionized water was used as the blank. Absorption peaks between 270 and 300 nm corresponded to the surface plasmon resonance of CuO NPs, confirming their successful formation [36].

2.6.2 FTIR spectroscopy analysis

Functional groups and molecular interactions were identified by FTIR analysis using a PerkinElmer Spectrum Two instrument in attenuated total reflectance (ATR) mode. Spectra were recorded from 4000 to 400 cm^{-1} with a resolution of 4 cm^{-1}, averaging 64 scans per sample. Characteristic peaks related to hydroxyl (O–H), carbonyl (C=O), amide groups, and metal–oxygen (Cu–O) vibrations confirmed nanoparticle integration into the scaffold matrix [37].

2.6.3 XRD analysis

Crystalline structure of CuO NPs and composite scaffolds was examined by XRD using a Bruker D8 Advance diffractometer with CuKα radiation (λ = 1.5406 Å), operated at 40 kV and 40 mA. Diffraction patterns were recorded from 2θ = 5° to 90° with a step size of 0.029649°. Sharp peaks corresponding to monoclinic CuO phases validated nanoparticle crystallinity, while peak shifts in the composites indicated successful embedding [38].

2.6.4 SEM imaging

Surface morphology and distribution of CuO NPs within the scaffolds were analyzed by SEM (JEOL JSM-IT800 NANO). Samples were sputter-coated with gold before imaging. Micrographs demonstrated uniform nanofibers with minimal bead formation and even nanoparticle dispersion [39].

2.6.5 TGA

Thermal stability was assessed using a PerkinElmer TGA 8000. Approximately 5 mg of sample was heated under nitrogen atmosphere from room temperature to 550°C at a heating rate of 15°C/min. Weight loss curves identified moisture evaporation, polymer degradation, and composite breakdown. CuO-containing scaffolds exhibited improved thermal resistance compared to controls [40].

2.6.6 DLS and zeta potential

Hydrodynamic diameter and surface charge of CuO NPs were measured with a Malvern Zetasizer Ultra. DLS analysis provided particle size distribution and polydispersity index (PDI), while zeta potential measurements assessed colloidal stability. Values exceeding ±30 mV indicated strong repulsive forces, supporting nanoparticle stability for biomedical applications [21].

All raw and processed data have been uploaded to the Mendeley Data repository (DOI: 10.17632/763h4wwkrj.2) for transparency and reproducibility.

2.7 *In vitro* anticancer activity

2.7.1 Cell lines procurement and culture

Human colon adenocarcinoma (HT-29) and breast cancer (MCF-7) cell lines were obtained from the National Center for Cell Science (NCCS), Pune, India. Cells were cultured according to supplied protocols in Minimum Essential Medium (MEM) supplemented with 10% fetal bovine serum (FBS) and incubated at 37°C in a humidified 5% CO_2 atmosphere [24].

2.7.2 MTT assay for cell viability

HT-29 and MCF-7 cells were seeded into 96-well plates at a density of 5×10^5 cells/well and allowed to adhere overnight. Cells were then exposed to varying concentrations (6.25, 12.5, 25, 50, and 100 µg/mL) of algal extract, CuO NPs, and starch/PVA/CuO nanoscaffolds, each tested in triplicate, for 24 hours at 37°C with 5% CO_2. After treatment, 20 µL of MTT solution was added per well and incubated for 4 hours. Formazan crystals formed were dissolved in 200 µL dimethyl sulfoxide (DMSO), and absorbance was measured at 570 nm using a microplate reader. The assay was repeated three times independently to confirm reproducibility. Mean optical density (OD) values and standard deviations were calculated [41].

2.8 Statistical analysis

All quantitative data were analyzed using SPSS version 25.0 and GraphPad Prism 9.0 software. Results from triplicate experiments are expressed as mean ± standard deviation (SD). One-way analysis of variance (ANOVA) followed by post-hoc tests (Tukey's or Dunnett's) was applied to assess significance between groups, with p-values < 0.05 considered statistically significant. Pearson correlation coefficients were calculated to determine relationships between variables. The Shapiro–Wilk test evaluated normality, and data not normally distributed were log-transformed. Statistical interpretations were made within a 95% confidence interval to ensure robustness [42].

3. RESULTS

3.1. UV–visible spectroscopy

The UV–Visible spectral assessment (Fig. 1) provided insights into the optical characteristics of both the *G. corticata* extract and the green-fabricated CuO NPs. The aqueous extract exhibited a broad absorption range from 200 nm to 800 nm, peaking prominently at 302 nm with an absorbance of 1.268. This broad spectral profile is characteristic of phytochemicals like polyphenols and flavonoids, which are responsible for reducing and stabilizing metal ions during nanoparticle formation. In contrast, the CuO NPs demonstrated a distinct surface plasmon resonance (SPR) peak centered at 291 nm, indicating the presence of nanoparticles due to the collective oscillation of conduction electrons. Additionally, the CuO NPs showed notable absorbance near 800 nm (1.200), decreasing progressively toward shorter wavelengths, which aligns with typical behavior of metal oxide nanoparticles. The absence of sharp features in the extract and the clear SPR peak in the nanoparticle sample confirm successful biosynthesis of CuO NPs mediated by the *G. corticata* extract as a natural reducing and capping agent [43, 44].

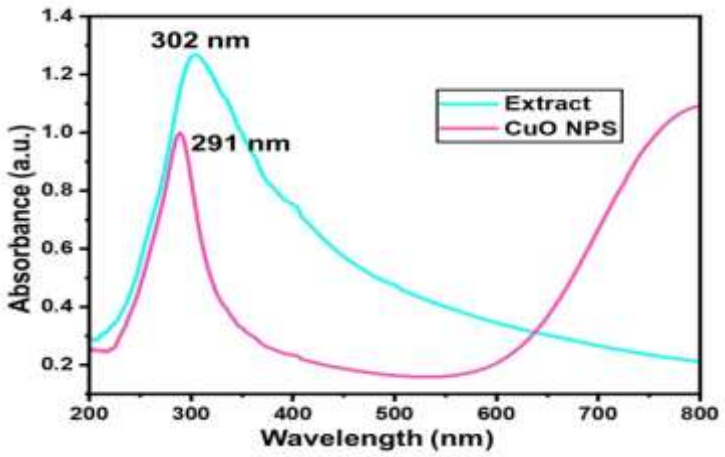

Fig. 1. UV–Visible spectral profiles of algal extract and CuO NPs.

3.2. FTIR spectroscopy analysis

FTIR spectra (Fig. 2) were recorded using a PerkinElmer Spectrum Two spectrometer in ATR mode to identify functional groups present in the CuO NPs and the nanoscaffold composite. The spectrum for CuO NPs showed prominent absorption bands related to O–H stretching vibrations and Cu–O bonds, confirming metal–oxygen linkage formation. The nanoscaffold spectrum revealed ten characteristic peaks, including a broad O–H stretch at 3303.50 cm^{-1}, a carbonyl C=O stretch at 1709.35 cm^{-1}, and aliphatic C–H stretching at 2924.80 cm^{-1}, alongside peaks at 1427.14, 1329.09, 1141.87, 1088.65, 919.75, 843.06, and 601.37 cm^{-1}, indicative of polymeric constituents like amides and polysaccharides. These spectral signatures demonstrate the successful incorporation of CuO NPs into the polymer matrix, with interactions likely via metal coordination and hydrogen bonding. The presence of bioactive groups derived from *G. corticata* suggests its role in stabilizing nanoparticles at the interface [45, 46].

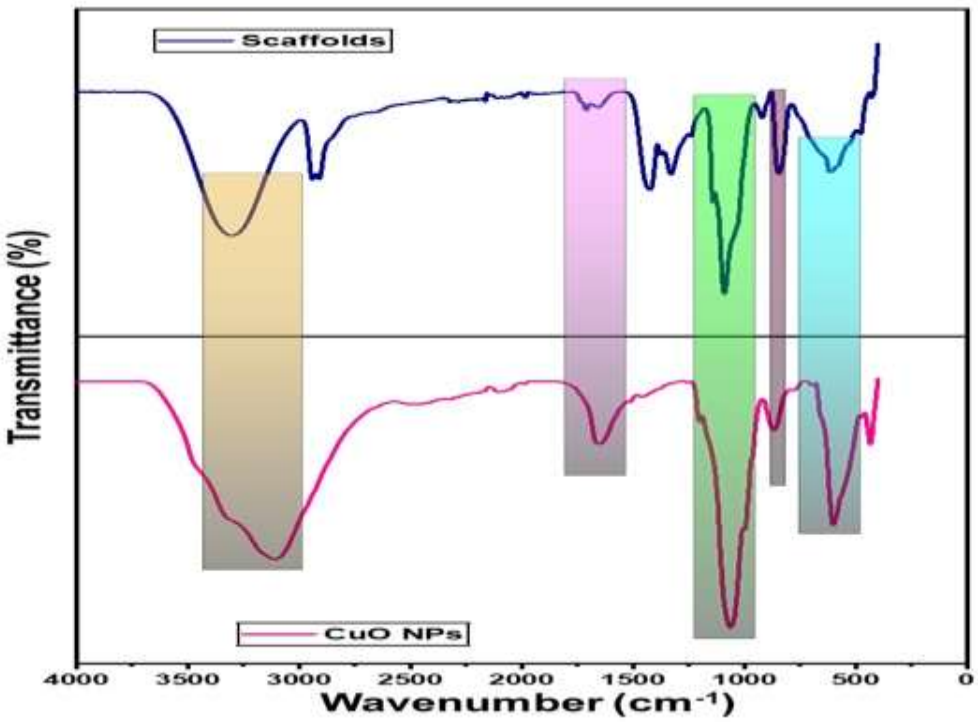

Fig. 2. FTIR spectra of CuO NPs and their incorporation into nanoscaffolds.

3.3. XRD analysis

XRD analysis (Fig. 3) using a Bruker D8 Advance diffractometer detailed the crystalline nature of the synthesized CuO NPs and the nanoscaffold composite. The CuO NPs exhibited 37 diffraction peaks within the 2θ range of 12.852° to 57.284°, with intense reflections at 19.134°, 24.369°, and 15.797°, which match monoclinic CuO as

per JCPDS card 48-1548. These reflections correspond to d-spacing values of 4.63468 Å, 3.64963 Å, and 5.60549 Å, confirming the crystalline purity of the nanoparticles. The nanoscaffold presented 13 diffraction peaks, notably at 29.445° and 21.346°, indicative of a semi-crystalline architecture composed of approximately 20.2% crystalline and 79.8% amorphous phases. Broadened peaks, such as the one at 43.067° with a full width at half maximum (FWHM) of 1.025°, suggested small crystallite sizes and effective dispersion of CuO NPs within the polymer. Minor peak shifts, like from 35.999° to 36.034°, implied strong interfacial bonding likely mediated by phytochemicals from the *G. corticata* extract, enhancing nanoparticle–polymer interactions [47, 48].

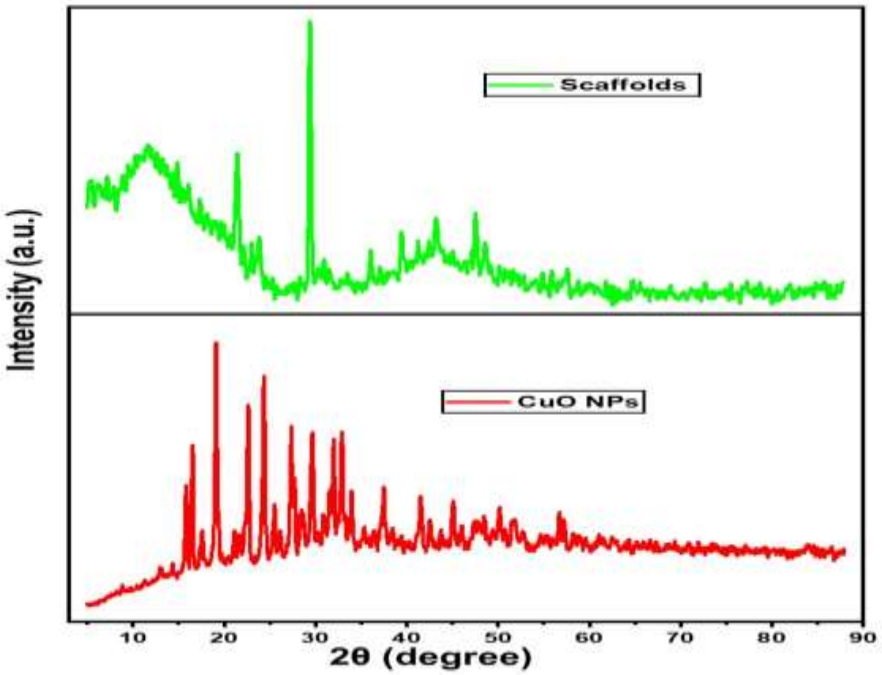

Fig. 3. XRD patterns of synthesized CuO NPs and CuO-loaded scaffolds.

3.4. SEM analysis

Morphological examination (Fig. 4) of CuO NPs embedded within electrospun starch/PVA nanoscaffolds was conducted using a JEOL JSM-IT800 NANO SEM system. Micrographs displayed a continuous network of fibers with smooth surfaces, measuring between 90 and 150 nm in diameter. The fibers were free of beads or defects, indicating successful electrospinning. Spherical CuO NPs, smaller than 100 nm, were homogeneously distributed across fiber surfaces and embedded within the scaffold without aggregation. This uniform dispersion confirms effective mixing of nanoparticles with the polymer solution prior to electrospinning. The preserved fibrous morphology confirms compatibility between CuO NPs and the starch/PVA matrix. The bioactive compounds in *G. corticata* extract likely contributed to nanoparticle stabilization and prevented agglomeration through natural capping effects [49].

3.5. TGA

TGA (Fig. 5) of the nanoscaffold, performed using a PerkinElmer thermal analyzer, involved heating from 30°C to 550°C at a rate of 15°C/min. The resulting thermogram revealed two principal degradation phases: the first initiating at 265.25°C and peaking at 355.41°C, attributed to the decomposition of organic residues and polymer components; the second phase starting at 425.38°C with a maximum degradation temperature of 448.38°C, associated with the breakdown of more thermally stable constituents. The total mass loss was 33.372%, illustrating the scaffold's thermal decomposition profile. The relatively high onset of degradation suggests enhanced thermal stability, likely due to CuO NP reinforcement and potential cross-linking within the polymer. Furthermore, secondary metabolites from *G. corticata* may contribute to improved thermal properties by interacting protectively with polymer chains [50, 51].

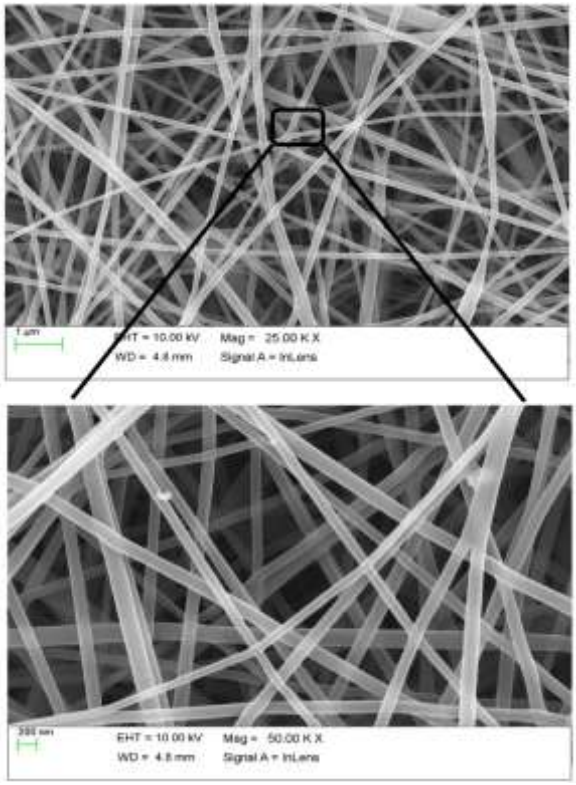

Fig. 4. SEM analysis of synthesized CuO NPs and CuO-loaded scaffolds.

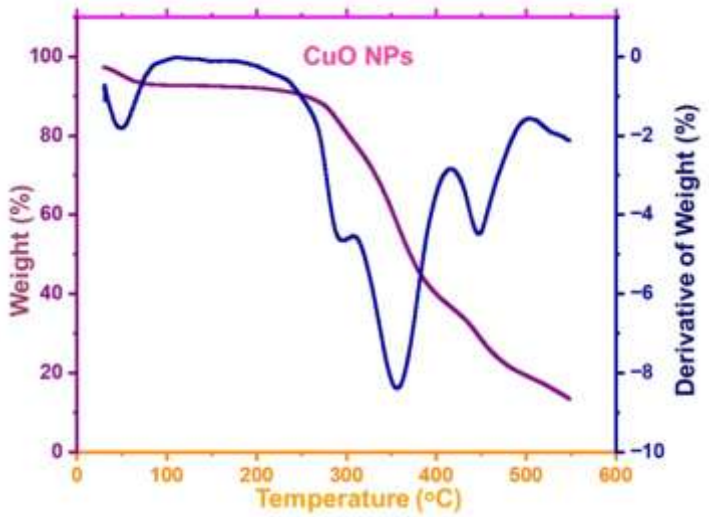

Fig. 5. Thermal degradation behavior of CuO-incorporated nanoscaffolds.

3.6. DLS and zeta potential analysis

The colloidal behavior of biosynthesized CuO NPs was characterized by DLS and zeta potential measurements using a Malvern Zetasizer. The nanoparticles exhibited a bimodal size distribution with an average hydrodynamic diameter (Z-average) of 68.6 nm (Fig. 6) and a polydispersity index (PDI) of 0.584, indicating moderate size heterogeneity. The zeta potential was recorded at -14.11 mV, with distribution peaks at -25.21 mV and -5.514 mV (Fig. 7), reflecting a moderately negative surface charge which confers partial colloidal stability. This negative charge is attributed to the biomolecules from the *G. corticata* extract adsorbed on the nanoparticle surface. Conductivity was measured at 0.05175 mS/cm, and the wall zeta potential registered -12.73 mV. While the observed values suggest reasonable dispersion stability, further surface modification may be necessary to optimize long-term stability, especially for biomedical applications that demand consistent nanoparticle behavior [52, 53].

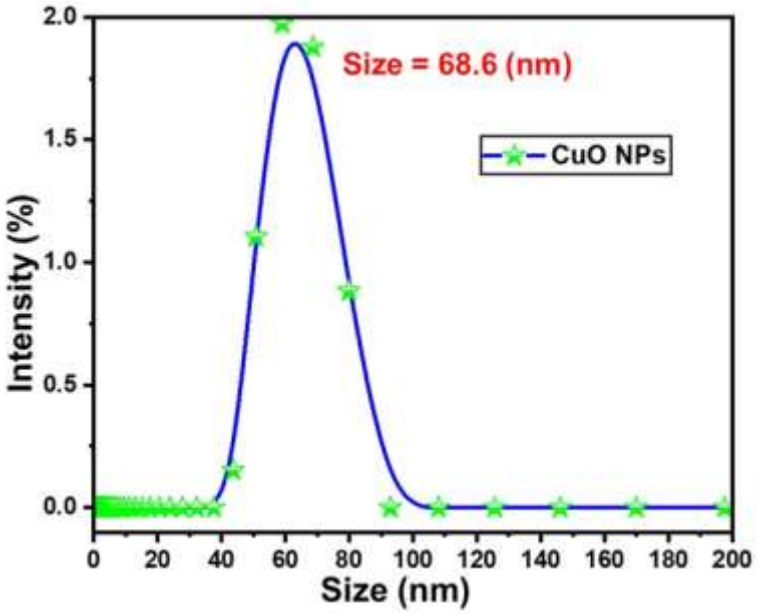

Fig.6. DLS particles size analysis of CuO NPs

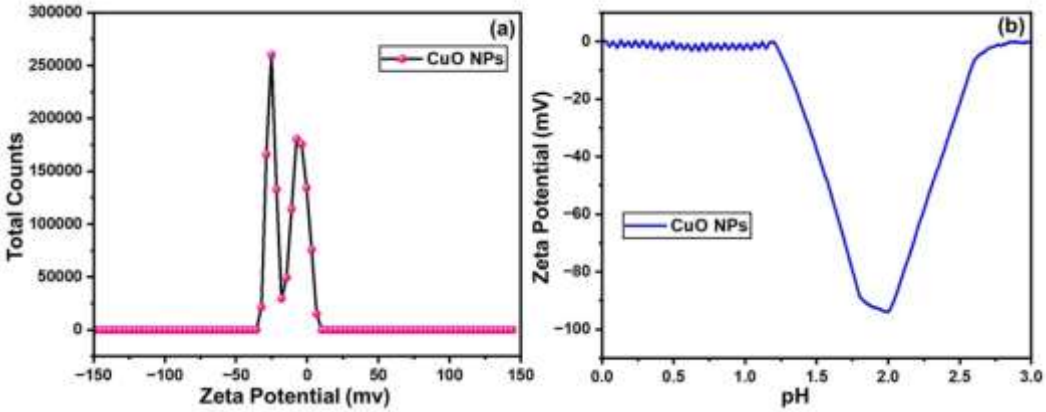

Fig.7. Zeta-potential analysis of CuO NPs

3.7. *In vitro* anticancer activity

The *in vitro* anticancer activity (Fig. 8) of the algal extract, CuO NPs, and starch/PVA/CuO-NPs nanoscaffolds was evaluated against HT-29 (colon adenocarcinoma) and MCF-7 (breast cancer) cell lines using the MTT assay. The results demonstrated concentration-dependent cytotoxicity in both cell lines, with the nanoscaffolds showing the most potent effects.

Against HT-29 cells, the algal extract exhibited moderate activity, reducing cell viability from 94.7% at 6.25 µg/mL to 33.45% at 100 µg/mL, with an estimated IC50 of approximately 50 µg/mL. CuO NPs displayed stronger cytotoxicity, decreasing viability from 79.7% to 23.03% over the same concentration range, yielding an IC50 of about 15 µg/mL. The starch/PVA/CuO-NPs nanoscaffolds were the most effective, suppressing viability to just 16.08% at 100 µg/mL and achieving an IC50 of roughly 10 µg/mL.

Similar trends were observed in MCF-7 cells. The algal extract reduced viability from 96.5% to 47.25%, with an IC50 near 40 µg/mL. CuO NPs showed enhanced activity, lowering viability from 86.0% to 38.67% and an IC50 of approximately 25 µg/mL. Once again, the nanoscaffolds outperformed the other treatments, reaching 25.62% viability at the highest concentration and an IC50 of about 20 µg/mL [54].

These findings indicate that the starch/PVA/CuO-NPs nanoscaffolds possess the strongest anticancer activity against both tested cell lines, followed by CuO NPs and then the algal extract. The enhanced efficacy of the nanoscaffolds suggests their potential as a promising therapeutic approach, warranting further investigation into their mechanisms and *in vivo* performance. The IC50 values, while informative, should be confirmed with additional experiments for precise quantification.

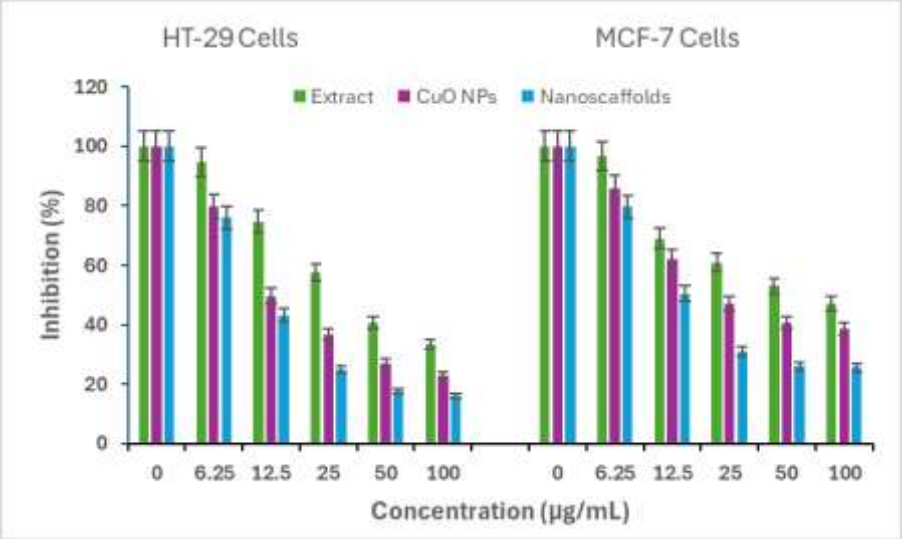

Fig. 8. Anticancer activity of algal extract, CuO-NPs and starch/PVA/CuO-NPs nanoscaffolds

4. DISCUSSION

The present study systematically evaluated the biosynthesis and characterization of CuO NPs using *G. corticata* extract and their incorporation into electrospun starch/PVA nanoscaffolds. Each characterization technique revealed critical insights into the structural, chemical, and biological behavior of the developed nanocomposite, validating its potential for biomedical applications, particularly anticancer therapy.

UV–Visible spectroscopic analysis provided foundational evidence for the successful biosynthesis of CuO NPs using *G. corticata* extract. The aqueous extract exhibited a wide absorption range between 200 and 800 nm, with a characteristic peak at 302 nm, suggesting the presence of bioactive phytochemicals such as polyphenols, flavonoids, and terpenoids. These compounds are known for their ability to donate electrons, facilitating the reduction of metal ions into stable nanoparticles. In comparison, the CuO NPs exhibited a pronounced absorption peak at 291 nm, indicative of surface plasmon resonance (SPR), a hallmark of nanoscale metal oxides. A secondary absorption was observed near 800 nm, further supporting the formation of metal oxide nanostructures. The absence of such defined peaks in the extract and their presence in the nanoparticle spectrum validate the extract's dual role as both reducing and capping agent during nanoparticle synthesis [55, 56].

FTIR spectroscopy was employed to identify the functional groups involved in nanoparticle formation and stabilization. The CuO NPs spectrum revealed key absorption bands attributable to O–H and Cu–O stretching, confirming metal-oxygen bonding. The spectrum of the nanoscaffold showed distinct peaks corresponding to hydroxyl (O–H), carbonyl (C=O), and aliphatic C–H bonds, along with signatures typical of polysaccharides and amide groups. The presence of such peaks implies effective incorporation of CuO NPs into the polymeric matrix, possibly through hydrogen bonding and electrostatic interactions. These interactions are facilitated by the phytochemicals from *G. corticata*, which likely enhance compatibility between the nanoparticles and the starch/PVA scaffold, stabilizing the system and preventing nanoparticle aggregation [57-61].

XRD patterns affirmed the crystalline nature of the synthesized CuO NPs. Multiple diffraction peaks matched the monoclinic phase of CuO, in alignment with JCPDS card no. 48-1548. The presence of sharp and well-defined peaks at 2θ values such as 19.134°, 24.369°, and 15.797° confirmed high crystallinity and phase purity. In contrast, the nanoscaffold composite exhibited broader and less intense peaks, reflecting a semi-crystalline structure with predominant amorphous content. Notably, a peak shift from 35.999° to 36.034° in the nanoscaffold indicated strong interfacial interactions between the CuO NPs and the polymer matrix, most likely mediated by the phytochemicals. These findings underscore the structural integration of the nanoparticles into the scaffold while maintaining their crystalline nature [62-65].

SEM imaging revealed the morphological characteristics of the electrospun nanoscaffold. The scaffold exhibited a continuous, bead-free fibrous network, with fiber diameters ranging from 90 to 150 nm, which is ideal for mimicking natural ECM. Embedded CuO NPs appeared as uniformly dispersed spherical entities under 100 nm, distributed both within and on the surface of the nanofibers. This uniform dispersion is crucial for consistent therapeutic activity and highlights the effective blending of nanoparticles with the polymer solution prior to electrospinning. The smooth surface and homogenous nanoparticle integration suggest excellent compatibility among the components, further aided by the stabilizing agents present in the algal extract [66-68].

Thermal stability of the nanoscaffold was evaluated through TGA. The thermogram displayed two major degradation phases. The first, occurring between 265.25°C and 355.41°C, corresponded to the decomposition of polymeric and organic residues. The second phase, from 425.38°C to 448.38°C, was attributed to the breakdown of more stable constituents, possibly cross-linked structures and embedded nanoparticles. The total weight loss was approximately 33.372%, indicating partial degradation, which is acceptable for biodegradable biomedical materials. The relatively high degradation onset temperature implies improved thermal resistance, likely due to nanoparticle reinforcement and potential cross-linking interactions induced by bioactive compounds in *G. corticata* [69, 70].

DLS and zeta potential analyses were performed to assess the colloidal stability and size distribution of the CuO NPs. The average hydrodynamic diameter was 68.6 nm with a polydispersity index (PDI) of 0.584, suggesting moderate uniformity in particle size. The zeta potential of −14.11 mV indicated moderate surface charge, which confers partial electrostatic stabilization. While these values reflect acceptable short-term stability, surface modifications or additional capping agents may be necessary for long-term dispersion, especially in complex biological environments. The negative surface charge likely originates from the phytochemical groups adsorbed onto the nanoparticles during green synthesis [71, 72].

The anticancer efficacy of the *G. corticata* extract, CuO NPs, and the starch/PVA/CuO nanoscaffolds was evaluated against HT-29 (colon) and MCF-7 (breast) cancer cell lines using the MTT assay. All treatments showed dose-dependent cytotoxicity, with the nanoscaffolds exhibiting the strongest activity. In HT-29 cells, the scaffold's IC50 was around 10 µg/mL, compared to 15 µg/mL for CuO NPs and 50 µg/mL for the extract. A similar trend was seen in MCF-7 cells, with IC50 values of 20 µg/mL for the scaffold, 25 µg/mL for CuO NPs, and 40 µg/mL for the extract. These findings highlight the synergistic effect of CuO NPs and polymeric support in enhancing anticancer activity. The improved performance of the scaffold can be attributed to better nanoparticle delivery and sustained interaction with cancer cells due to the nanofibrous matrix [74, 74].

The comprehensive results from physicochemical and biological evaluations validate the successful green synthesis of CuO NPs using *G. corticata* and their efficient integration into a starch/PVA nanoscaffold. The material demonstrated favorable structural, thermal, and anticancer properties, suggesting promising potential for future biomedical applications, particularly in targeted cancer therapy.

5. CONCLUSION

The present study successfully demonstrated the green synthesis of copper oxide (CuO) nanoparticles using *G. corticata* extract, which served as both a reducing and stabilizing agent. The UV–Vis, FTIR, and XRD analyses confirmed the formation and crystalline nature of the CuO NPs, while SEM imaging revealed their uniform dispersion within the starch/PVA electrospun nanoscaffold. The incorporation of CuO NPs enhanced the scaffold's thermal stability and maintained its structural integrity. DLS and zeta potential analyses indicated moderate colloidal stability, influenced by the phytochemicals present in the algal extract. Most importantly, the *in vitro* anticancer evaluation showed that the CuO-loaded nanoscaffolds exhibited significant cytotoxicity against HT-29 and MCF-7 cancer cell lines, outperforming both the extract and nanoparticles alone. These findings highlight the therapeutic potential of the fabricated nanoscaffolds as a biocompatible and eco-friendly platform for targeted cancer therapy, paving the way for further *in vivo* evaluations and clinical exploration.

Ethics declaration: Not Applicable

Conflicts of Interest: The authors declare no conflicts of interest.

Data Availability Statement: The full dataset of physiochemical characterization associated with this work is published in Mendeley Data **[Dataset]** Sustainable nanohybrid systems: Physiochemical properties of *Gracilaria corticota* extract-mediated copper oxide nanoparticle-loaded starch scaffolds (DOI: 10.17632/763h4wwkrj.1). Disclosure: The material characterization data and figures (e.g., UV, SEM, FTIR, XRD, TGA, Zeta Potential and particle sizer) presented here were generated from a common dataset and are being reused across multiple related studies on nanomaterials. All biological analyses and conclusions are original to each manuscript.

REFERENCES

[1] Rajendran MS, Jayaraman S, Khan JM, Jasmine S, Prabhakaran RK, Raju MV, Chandrasekaran MK, Ahalliya RM, Kannappan P, Palanisamy CP, Kanniappan GV. Investigating the colon toxicity and carcinogenic role of monosodium glutamate compared with Dimethylhydrazine in male Wistar rats: Exploring the link to childhood colon cancer risk. Journal of King Saud University - Science. 2024; 36(11): 103507.

[2] Kumarasamy RV, Natarajan P, Umapathy VR, Roy JR, Rab SO, Saeed M, Panagal M, Mironescu M, Srinivasan GP, Palanisamy CP. Clinical Applications and Therapeutic Potentials of Advanced

Nanoparticles: A Comprehensive Review on Completed Human Clinical Trials. Frontiers in Nanotechnology. 2024; 6:1479993.
[3] Jin W, Pei JJ, Roy JR, Jayaraman S, Ahalliya RM, Kanniappan GV, Mironescu M, Palanisamy CP. Comprehensive review on single-cell RNA sequencing: A new frontier in Alzheimer's disease research. Ageing Research Reviews. 2024; 274: 102454.
[4] Pei J, Palanisamy CP, Jayaraman S, Natarajan PM, Umapathy VR, Roy JR, Panagal M, Jayaraman S. Curcumin-loaded polymeric nanomaterials as a novel therapeutic strategy for Alzheimer's disease: A comprehensive review. Ageing Research Reviews. 2024; 99: 102393.
[5] Pei J, Palanisamy CP, Jayaraman S, Natarajan PM, Umapathy VR, Roy JR, Thalamati D, Ahalliya RM, Kanniappan GV, Mironescu M. A comprehensive review on starch-based Sustainable Edible Films Loaded with Bioactive Components for Food Packaging. International Journal of Biological macromolecules. 2024; 274 (Part-1): 133332.
[6] Palanisamy CP, poompradub S, Sansanaphongpricha K, Subramani K, Sonsudin F. Increased expression levels of PDGF and VEGF magnify the wound healing potential facilitated by biogenic synthesis of silver nanoparticles. Nano-Structures & Nano-Objects. 2024; 39: 101236.
[7] Pei J, Palanisamy CP, Jayaraman S, Natarajan PM, Umapathy VR, Roy JR, Thalamati D, Ahalliya RM, Kanniappan GV, Mironescu M. Proteomics Profiling of Extracellular Vesicle for Identification of Potential Biomarkers in Alzheimer's Disease: A Comprehensive Review. Ageing Research Reviews. 2024; 99: 102359.
[8] Xi J, Wang T, Xian P, Liu X, Du M, Yang H, Palanisamy CP, Lin W, Long Q. Proteomic insights uncover enhanced neurotherapeutic potential in conditioned mesenchymal stem cell-derived extracellular vesicles. Extracellular Vesicle. 2024; 3: 100037.
[9] Pei J, Natarajan PM, Umapathy VR, Swamikannu B, Sivaraman NM, Krishnasamy L, Palanisamy CP. Advancements in the synthesis and functionalization of zinc oxide-based nanomaterials for enhanced oral cancer therapy. Molecules. 2024; 29(11): 2706.
[10] Gatasheh MK, Natarajan SR, Krishnamoorthy R, Alsulami TS, Rajagopal P, Palanisamy CP, Veeraraghavan VP, Jayaraman S. Molecular analysis to identify novel potential biomarkers as drug targets in colorectal cancer therapy: an integrated bioinformatics analysis. Molecular and Cellular Oncology. 2024; 11(1): 2326699.
[11] Pei J, Yan Y, Jayaraman S, Rajagopal P, Natarajan PM, Umapathy VR, Gopathy S, Roy JR, Sadagopan CS, Thalamati D, Palanisamy CP, Mironescu M. A review on advancements in the application of starch-based nanomaterials in biomedicine: Precision drug delivery and cancer therapy. International Journal of Biological Macromolecules. 2024; 130746.
[12] Pei JJ, Yan Y, Palanisamy CP, Jayaraman S, Natarajan PM, Umapathy VR, Gopathy S, Roy JR, Sadagopan JC, Thalamati D, Mironescu M. Materials-based drug delivery approaches: Recent advances and future perspectives. Green Processing and Synthesis. 2024; 13: 20230094.
[13] Pei JJ, Deng W, Liu Y, Guo Y, Chen J, Abdu H, Khan MR, Palanisamy CP, El-Aty AM. A Comprehensive Review of Cornus officinalis: Health Benefits, Phytochemistry, and Pharmacological Effects for Functional Drug and Food Development. Frontiers in Nutrition. 2023; 10: 1309963.
[14] Alugoju P, Palanisamy CP, Anthikapalli NVA, Jayaraman S, Prasanskulab A, Chuchawankul S, Dyavaiah M, Tencomnao T. Exploring the anti-aging potential of natural products and plant extracts in budding yeast Saccharomyces cerevisiae: A review. F1000Research. 2023; 12: 1265.
[15] Lavanya M, Krishnamoorthy R, Alshuniaber MA, Manoharadas S, Palanisamy CP, Veeraraghavan VP, Jayaraman S, Rajagopal P, Padmini R. Formulation, characterization and evaluation of gelatin-syringic acid/zinc oxide nanocomposite for its effective anticancer, antioxidant and anti-inflammatory activities. Journal of King Saud University-Science. 2023; 35: 102909.
[16] Palanisamy CP, Poompradub S, Sansanaphongpricha K, Jayaraman S, Subramani K, Sonsudin F. Biosynthesis of silver nanoparticles (AgNPs) using ethanolic extract of Nigella sativa (L.) seeds promotes wound healing via PDGF and VEGF signalling pathways activation. Biocatalysis and Agricultural Biotechnology. 2023; 54: 102970.
[17] Prasad M, Jayaraman S, Natarajan SR, Veeraraghavan VP, Krishnamoorthy R, Gatasheh MK, Palanisamy CP, Elrobh M. Piperine modulates IR/Akt/GLUT4 pathways to mitigate insulin resistance: Evidence from animal and computational studies. International Journal of Biological Macromolecules. 2023; 253: 127242.
[18] Palanisamy CP, Pei JJ, Phaniendra A, Venkata AAN, Jayaraman S, Veeraragahavan VP, Sridevi G, Roy JR, Janaki CS, Thalamati D, Mironescu M, Luo Q, Chai Y, Long Q. New Strategy of Neurodegenerative Disease Treatment with Extracellular Vesicles (EVs) Derived from Mesenchymal Stem Cells (MSCs). *Theranostics*. 2023; 13(12):4138-4165. doi:10.7150/thno.83066.
[19] Palanisamy CP, Phaniendra A, Jayaraman S, Poompradub S. *Nigella sativa* L. seed extracts promotes wound healing progress by activating VEGF and PDGF signalling pathways: *An in vitro* and *in silico* study. *F1000 Research*. 2023; 12: 436.

[20] Pei JJ, Palanisamy CP, Phaniendra A, Venkata AAN, Natarajan PM, Umapathy VR, Swamikannu B, Jayaraman S, Rajagopal P, Poompradub S. A comprehensive review on bio-based materials for chronic diabetic wounds. *Molecules*. 2022; 28(2), 604.
[21] Perumal MKK, Renuka RR, Subbiah SK, Natarajan PM. Artificial intelligence-driven clinical decision support systems for early detection and precision therapy in oral cancer: a mini review. Frontiers in Oral Health. 2025; 6: 1592428.
[22] Ramesh E, Ganesan A, Lakshmi KC, Natarajan PM. Artificial intelligence-based diagnosis of oral leukoplakia using deep convolutional neural networks Xception and MobileNet-v2. Frontiers in Oral Health. 2025; 6: 1414524.
[23] Ganesan A, Kumar NG, Natarajan PM. Anticancer activity of silver nanoparticles synthesized from aqueous leaf extract of Solanum trilobatum (Purple fruit pea eggplant) on human oral cancer cells. Journal of Herbmed Pharmacololgy. 2024; 13(2): 260-268.
[24] Natarajan PM, Swamikannu B, Sivaraman NM, Stylin AGSQ. Prevention of Oral Cancer: A Comprehensive Guide. Journal of Pharmacy and Bioallied Sciences. 2024; 16(5): S4239-S4241.
[25] Umapathy V, Dhanavel A, Kesavan R, Natarajan PM, Bhuminathan S, Vijayalakshmi P. Anticancer Potential of the Principal Constituent of Piper nigrum, Piperine: A Comprehensive Review. Cureus. 2024; 16(2): e54425.
[26] Umapathy VR, Swamikannu B, Natarajan PM, Devi R, Nandini MS, Vimalarani, Vijayalakshmi P. In Silico Molecular Docking of Ocimum sanctum Phytochemicals: Targeting Key Biomarkers in Oral Cancer. Journal of Pharmacy and Bioallied Sciences. 2024; 16(5): S4792-S4799.
[27] Natarajan PM, Bhuminathan S, Rajan R, Bindu K, Loganathan K, Veerakumar R. The Crucial Role of Smoking Cessation in Preventing Oral Cancer. Journal of Pharmacy and Bioallied Sciences. 2024; 16(5): S4245-S4247.
[28] Swamikannu B, Umapathy VR, Natarajan PM, Nandini MS, Stylin AGSQ, Vimalarani V, Rajinikanth S. Unlocking the Therapeutic Benefits of Artemisia Annua: A Comprehensive Overview of its Medicinal Properties. Journal of Pharmacy and Bioallied Sciences. 2024; 16(5): S4248-S4253.
[29] Natarajan PM. Computational Studies on Recent Congeners of Fluoroquinolones and Nitroimidazoles for Their Use in Periodontal Therapy. Journal of Pharmacy and Bioallied Sciences. 2024; 16(5): S4731-S4740.
[30] Yadalam PK, Arumuganainar D, Natarajan PM, Ardila CM. Artificial intelligence-powered prediction of AIM-2 inflammasome sequences using transformers and graph attention networks in periodontal inflammation. Scientific Reports. 2025; 15: 8733.
[31] Yadalam PK, Chatterjee S, Natarajan PM, Ardila CM. Comparison of light gradient boosting and logistic regression for interactomic hub genes in Porphyromonas gingivalis and Fusobacterium nucleatum-induc ed periodontitis with Alzheimer's disease. Frontiers in Oral Health. 2025; 6:1463458.
[32] Natarajan PM, Bhuminathan S, Leela B, Bindu K, Loganathan K, Ramachandran V. Smoking and its Role in Oral Cancer. Journal of Pharmacy and Bioallied Sciences 16(5): S4242-S4244.
[33] Yadalam PK, Natarajan PM, Ardila CM. Variational graph autoencoder for reconstructed transcriptomic data associated with NLRP3 mediated pyroptosis in periodontitis. Scientific Reports. 2025; 15: 1962.
[34] Daniel Raja FS, Abraham L, Rangasamy K, Saikia K, Rathankumar AK, Mironescu M, Mironescu I, Palanisamy CP, Kanniappan GV. Next-Generation Microbiome Therapeutics: Psychobiotics and Fecal Microbiota Transplants (FMT) for Mental Health Treatment. Frontiers in Cellular and Infection Microbiology. 2026; 16: 1719357.
[35] Dharmaprakash S, Gunasekaran VP, Sivaramakrishnan R, Kanniappan GV, Jayaraman S, Mironescu M, Rajabathar JR, Mironescu ID, Palanisamy CP. Marine macroalgae-mediated ultrasonic-assisted green synthesis of CuO nanoparticles embedded in starch/PVA electrospun nanoscaffolds for in vitro α-amylase and α-glucosidase inhibitory activity. Scientific Reports. 2026.
[36] Surendran N, Chandrasekaran G, Raju MV, Chandrasekaran MK, Ahalliya RM, Palanisamy CP, Kanniappan GV, Arcot R, Alharbi NS, Thiruvengadam M. Anti-inflammatory potential of ethanolic extract of Maranta arundinacea L.: Insights from COX-2 modulation and oxidative stress analysis. South African Journal of Botany. 2026; 195: 142-151.
[37] Pei J, Senthilkumar MV, Hessini K, Subramaniyam S, Sivaramakrishnan R, Kanniappan GV, Jayaraman S, Palanisamy CP. Green fabrication of starch/PVA/CuO nanoscaffolds using marine macroalgae extract for enhanced anti-inflammatory activity. Sustainable Chemistry and Pharmacy. 2026; 51: 102397.
[38] Balasubramanian V, Loganathan L, Muthuswamy K, Viswanathan TM, Raju MV, Chandrasekaran MK, Ahalliya RM, Poorasamy J, Palanisamy CP, Dominic S, Kanniappan GV. Anticancer therapeutic efficacy of PEGylated β-galactosidase from Aspergillus terreus in DMBA-induced breast cancer: Toxicological, molecular and histopathological evaluation in Wistar rats. International Journal of Biological Macromolecules. 2026; 360: 151856.
[39] Jayaraman S, Eswaran A, Rajagopal P, Palanisamy CP, Veerakumar P, Veeraraghavan VP, Sirasanagandla SR. Neuroendocrine-associated epigenetic factors in cellular senescence: mechanisms and therapeutic implications. Biogerontology. 2026; 27(2): 64.

[40] Ponnusamy B, Rajagopal P, Palanisamy CP, Veeraraghavan VP, Jayaraman S. Mechanistic Exploration of the anticancer activity of Justicia adhatoda Plant Leaf Ethanolic Extract against Colon Cancer Cells: An in silico and in vitro Approach. Asian Pacific Journal of Cancer Prevention. 2026; 27(3): 1069-1080.
[41] Pei J, Saran VS, Sivaramakrishnan R, Kanniappan GV, Pandurangan V, Jayaraman S, Dhayalan VK, Mironescu M, Mironescu ID, Palanisamy CP. Ultrasonic-assisted, Sargassum ilicifolium (brown marine macroalgae)-mediated biogenic synthesis of CuO nanoparticles incorporated in starch/PVA electrospun nanoscaffolds: In vitro safety and antioxidant efficacy assessment. Bioorganic Chemistry. 2026; 173: 109679.
[42] Raj MAPA, Subramaniyam S, Kanniappan GV, Jayaraman S, Palanisamy CP. Sustainable fabrication of starch/PVA/CuO electrospun nanoscaffolds from Turbinaria ornata (marine macroalgae) extract: Physicochemical characterization and antidiabetic evaluation. Kuwait Journal of Science. 2026; 53(2): 100545.
[43] Pei J, Ganesh NS, Subramaniyam S, Sivaramakrishnan R, Kanniappan GV, Jayaraman S, Palanisamy CP. Sustainable fabrication of starch/PVA/CuO electrospun nanoscaffolds from Padina tetrastromatica (Brown macroalgae) extract: Physicochemical characterization and antidiabetic assessment. Sustainable Chemistry One World. 2026; 9: 100195.
[44] Sakthiraj A, Sivaramakrishnan R, Subramaniyam S, Kanniappan GV, Pandurangan V, Jayaraman S, Dhayalan VK, Mironescu M, Mironescu ID, Palanisamy CP. Starch/PVA electrospun nanoscaffolds loaded with ultrasonic-assisted green-synthesis of CuO nanoparticles from marine macroalgae (Gracilaria corticata) extract: Cytotoxicity and antioxidant analysis. Chemical Physics Impact. 2026; 12: 101018.
[45] Raju M, Chandrasekaran MK, Loganathan L, Ahalliya RM, Mironescu M, Mironescu ID, Palanisamy CP, Kanniappan GV. Lipid remodeling and ferroptosis in phosphatidylcholine-mediated tumor–stroma crosstalk. Frontiers in Molecular Biosciences. 2026; 13: 1742305.
[46] Kunamalla R, Panagal M, Palanisamy CP. Biogenic synthesis and fabrication of starch/PVA/CuO electrospun nanoscaffolds from Sargassum ilicifolium (brown marine macroalgae) extract for anticancer activity on HT-29 and MCF-7 cancer cells. Biocatalysis and Agricultural Biotechnology. 2026; 72: 103923.
[47] Pei J, Govindaraj H, Sivaramakrishnan R, Kanniappan GV, Pandurangan V, Dhayalan VK, Mironescu M, Mironescu ID, Jayaraman S, Palanisamy PC. Sustainable fabrication of biopolymer-based (starch/PVA) nanoscaffolds loaded with green-synthesized CuO nanoparticles from Sargassum wightii (marine macroalgae): Cytocompatibility and antioxidant activity. Biomaterials Advances. 2026; 182: 214660.
[48] Pei J, Perumal NC, Meng P, Long Q, Palanisamy CP. Extracellular vesicle-based biosensors for Alzheimer's disease: A new frontier in precision diagnostics. Ageing Research Reviews. 2026; 113: 102904.
[49] Shree P, Sivaramakrishnan R, Kanniappan GV, Pandurangan V, Jayaraman S, Dhayalan VK, Mironescu M, Mironescu ID, Palanisamy CP. Antioxidant and biocompatible CuO-starch/PVA nanoscaffolds via ultrasonic green synthesis using Turbinaria conoides (brown marine macroalgae). Medicine in Drug Discovery. 2025; 28: 100238.
[50] Gong J, Lin J, Guan T, Pei J, Palanisamy CP, El-AtyFrom AMA. selenium tolerance to nanoplastic antagonism: Comprehensive characterization of L. casei SNUT1 and its extracellular vesicle–nanoselenium complex. Food Bioscience. 2025; 74: 107749.
[51] Poochi SP, Sundarraj R, Raju MV, Chandrasekaran MK, Ahalliya RM, Palanisamy CP, Kanniappan GV, Kondapavuluri BK, Thiruvengadam M. Harnessing Nature: Computational and Experimental Insights Into *Ipomoea obscura* Metabolites for Bladder Cancer Therapy. Chemistry and Biodiversity. 2025; 0: e00909.
[52] Dugganaboyana GK, Kannankumar MKG, Shivaramakrishna S, Raju MV, Chandrasekaran MK, Ahalliya RM, Panneerselvam N, Palanisamy CP, Kanniappan GV. Phytochemical insights, antioxidant activity and therapeutic potential of Cassia senna against prostate cancer in Wistar albino rats. Discover Applied Sciences. 2025; 7:1206.
[53] Natarajan SR, Krishnamoorthy R, Alshuniaber MA, Gatasheh MK, Rajagopal P, Veeraraghavan VP, Palanisamy CP, Jayaraman S. KDM1A Facilitates Oncogenic Potential in Colorectal Cancer Progression Through the Activation of AXIN/GSK3β/β-Catenin Signaling Pathways: Evidence From Integrated Transcriptomics and In Vitro Studies. The Journal of Gene Medicine. 2025; 27(11): e70053.
[54] Guan T, Gong J, Lin J, Palanisamy CP, Jinjin Pei J, El-Aty AMA. Machine learning-driven multimodal optimization of selenium biotransformation and flavor profiling in fermented apple–Yacon functional beverages. Innovative Food Science & Emerging Technologies. 2025; 105: 104198.
[55] Natarajan SR, Krishnamoorthy R, Alshuniaber MA, Alsulami TS, Gatasheh MK, Rajagopal P, Palanisamy CP, Govindan R, Veeraraghavan VP, Jayaraman S. ABCE1 facilitates tumour progression via aerobic glycolysis and inhibits cell death in human colorectal cancer cells through the p53 signalling pathway. Scientific Reports. 2025; 15: 24674.
[56] Huang Y, Guo H, Liu Y, Jin W, Palanisamy CP, Pei J, Oz F, El-Aty AMA. Effects of Natural Polysaccharides on the Gut Microbiota Related to Human Metabolic Health. Molecular Nutrition & Food Research. 2025; 69:e202400792.
[57] Poornima K, Meenakshi K.C, Manikandan V.R, Shankari G, Prabhu D, Rathi M.A, Palanisamy CP, Balaji

R, Gopalakrishnan V.K. Exploring the anticancer potential of Jerantinine A from *Tabernaemontana coronaria* against prostate, breast, and ovarian cancers: A computational approach. *Journal of Complementary and Integrative Medicine*, 2025 22(2): 363–372.
[58] Palanisamy CP, Poompradub S, Sansanaphongpricha K, Jayaraman S, Subramani K. Faridah Sonsudin gGreen synthesis of Nigella sativa-mediated silver nanoparticles for enhanced antibacterial activity and wound healing: Mechanistic insights and biomedical applications. Environmental Nanotechnology, Monitoring & Management. 2025; 24: 101085.
[59] Surendran N, Raju MV, Chandrasekaran MK, Ahalliya RM, Palanisamy CP, Chandrasekaran G, Kanniappan GV. Physicochemical characterization of starch from Maranta arundinacea L.(arrowroot) rhizomes and its inhibition of COX-2: In vivo validation. Bioactive Carbohydrates and Dietary Fibre. 2025; 33: 100465.
[60] Kannappan P, Chandrasekaran MK, Raju MV, Gopalakrishnan S, Dhamodharan P, Ahalliya RM, Palanisamy CP, Raju B, Kanniappan GV. Exploring the anticancer potential of Jerantinine A from Tabernaemontana coronaria against prostate, breast, and ovarian cancers: a computational approach. Journal of Complementary and Integrative Medicine. 2025; 22(02): 363-372.
[61] Pei J, Kumarasamy RV, Jayaraman S, Kanniappan GV, Long Q, Palanisamy CP. Quercetin-functionalized nanomaterials: Innovative therapeutic avenues for Alzheimer's disease management. Ageing Research Reviews. 2025; 104: 102665.
[62] Jayaraman S, Prasad M, Natarajan SR, Krishnamoorthy R, Alshuniaber MA, Gatasheh MK, Veeraraghavan VP, Rajagopal P, Palanisamy CP. Molecular mechanisms underlying the effects of beta-sitosterol on TGF-β1/Nrf2/SIRT1/p53-mediated signaling in the kidney of a high-fat diet and sucrose-induced type-2 diabetic rat. Chemico-Biological Interactions. 2025; 411: 111443.
[63] Huang Y, Guo H, Liu Y, Jin W, Palanisamy CP, Pei J, Oz F, El-Aty AMA. Effects of Natural Polysaccharides on the Gut Microbiota Related to Human Metabolic Health. Molecular Nutrition & Food Research. 2025; e202400792.
[64] Prabhakaran P, Palanisamy CP, Shanmugam A, Damodharan P, Swaminathan H, Devaraj D, Ahalliya RM, Kanniappan GV. Isolation, structural characterization, and molecular docking studies on the bioactive compound from n-Hexane extract of Emilia sonchifolia (L.) DC against the pancreatic cancer target Aurora 2 Kinase. Journal of Complementary and Integrative Medicine. 2024; 22(1): 0290.
[65] Jiang H, Kumarasamy RV, Pei J, Raju K, Kanniappan GV, Palanisamy CP. Integrating engineered nanomaterials with extracellular vesicles: Advancing targeted drug delivery and biomedical applications. Frontiers in Nanotechnology. 2024; 6: 1513683.
[66] Guo H, Liu Y, Wan T, Song D, Palanisamy CP, Geng J, Pei J, Özmen S, El-Aty AMA. Toward personalized cancer management: Role of precision nutrition–diet interventions. Journal of Functional Foods. 2024; 123: 106584.
[67] Natarajan SR, Krishnamoorthy R, Alshuniaber MA, Al-Anazi KM, Farah MA, Rajagopal P, Palanisamy CP, Veeraraghavan VP, Jayaraman S. Identification of FOXM1 as a novel protein biomarker and therapeutic target for colorectal cancer progression: Evidence from immune infiltration and bioinformatic analyses. International Journal of Biological Macromolecules. 282 (Part 4): 137201.
[68] Natarajan PM, Umapathy VR, Murali A, Swamikannu B. (2022). Computational Simulations of Identified marine-derived Natural Bioactive Compounds As Potential Inhibitors of Oral Cancer. Future Science OA. 2022; 8(3).
[69] Natarajan PM, Umapathy VR. Role of transcriptomics in the study of oral cancer. Frontiers in Oral Health. 2025; 6:1524364.
[70] Vidhyarekha U, Natarajan PM, Bhuminathan S, Sabarinathan J, Suba R, Vijayalakshmi P. Role of artificial intelligence in Oral Cancer. Advances in Public Health. 2024. 2024: 3664408.
[71] Ganesan A, Kumar NG, Natarajan PM, Gauthaman J. Automated classification of elongated styloid processes using deep learning models-an artificial intelligence diagnostics. Frontiers in Oral Health. 2025; 5: 1424840.
[72] Umapathy VR, Natarajan PM, Swamikannu B. Regenerative Strategies in Dentistry: Harnessing Stem Cells, Biomaterials and Bioactive Materials for Tissue Repair. Biomolecules. 2025; 15: 546.
[73] Natarajan PM. Dental Bioinformnatics-Current Scope and Future perspectives. Research Journal of Pharmacy and Technology. 2022;15(5):2351-6.
[74] Ganesan A, Kumar NG, Natarajan PM. Solanum trilobatum leaf extract-derived silver nanoparticles downregulate the PI3K/AKT/mTOR signaling pathway and attenuate oral squamous cell carcinoma cell proliferation. Journal of Herbmed Pharmacology. 2024; 13(2): 300-307.